CMS Physics Analysis Summary

Contact: cms-pag-conveners-bphysics@cern.ch 2017/05/15

Precision lifetime measurements of b hadrons reconstructed in final states with a J/ψ meson

The CMS Collaboration

Abstract

We present measurements of the lifetimes of the B^0, B_s^0, Λ_b^0, and B_c^+ hadrons using the decay channels $B^0 \to J/\psi K^*(892)^0$, $B^0 \to J/\psi K_S$, $B_s^0 \to J/\psi\pi^+\pi^-$, $B_s^0 \to J/\psi\phi(1020)$, $\Lambda_b^0 \to J/\psi\Lambda$, and $B_c^+ \to J/\psi\pi^+$. The data sample, corresponding to 19.7 fb^{-1}, was collected from proton-proton collisions at $\sqrt{s} = 8$ TeV using dedicated triggers to select oppositely charged muons in the J/ψ mass region. The lifetimes times the speed of light are measured to be

$$
\begin{aligned}
c\tau_{B^0} &= 453.0 \pm 1.6\ (\text{stat}) \pm 1.5\ (\text{syst})\ \mu\text{m}\ (\text{in}\ J/\psi K^*(892)^0)\\
c\tau_{B^0} &= 457.8 \pm 2.7\ (\text{stat}) \pm 2.7\ (\text{syst})\ \mu\text{m}\ (\text{in}\ J/\psi K_S)\\
c\tau_{B_s^0} &= 504.3 \pm 10.5\ (\text{stat}) \pm 3.7\ (\text{syst})\ \mu\text{m}\ (\text{in}\ J/\psi\pi^+\pi^-)\\
c\tau_{B_s^0} &= 443.9 \pm 2.0\ (\text{stat}) \pm 1.2\ (\text{syst})\ \mu\text{m}\ (\text{in}\ J/\psi\phi(1020))\\
c\tau_{\Lambda_b^0} &= 443.1 \pm 8.2\ (\text{stat}) \pm 2.7\ (\text{syst})\ \mu\text{m}\\
c\tau_{B_c^+} &= 162.3 \pm 8.2\ (\text{stat}) \pm 4.7\ (\text{syst}) \pm 0.1(\tau_{B^+})\ \mu\text{m}
\end{aligned}
$$

where the first uncertainty is statistical and the other is systematic. All results are in agreement with the current world average values.

1 Introduction

Precise lifetime measurements play an important role in the study of non-perturbative aspects of Quantum Chromodynamics (QCD). This phenomenology is commonly described by the QCD inspired Heavy Quark Expansion (HQE) model, which provides accurate estimates of the ratio of lifetimes for hadrons containing a common heavy quark. In this analysis we report a measurement of the lifetimes of the B^0, B^0_s, B^+_c mesons, and the Λ^0_b baryon.

The lifetime measurements are based on the reconstruction of the transverse decay length L_{xy}, where L_{xy} is defined as the flight distance vector from the production to the decay vertex of the b hadron projected on the transverse component (perpendicular to the beam axis) of the b hadron momentum p_T [1]. The proper decay time of the b hadron times the speed of light is calculated as

$$ct = \frac{L_{xy}}{(\beta\gamma)_T} = L_{xy}\frac{M}{p_\mathrm{T}}, \tag{1}$$

where M is the world average value of the mass of the b hadron.

The general approach in this work is to reconstruct the b hadrons in decays with a J/ψ in the final state, recorded by the CMS detector [2] using dedicated triggers that require two oppositely charged muons consistent with originating from a common vertex and with an invariant mass compatible with the J/ψ mass. Specifically, we reconstruct the decay chains $\mathrm{B}^+ \to \mathrm{J}/\psi\mathrm{K}^+$, $\mathrm{B}^0 \to \mathrm{J}/\psi\mathrm{K}^*(892)^0$, $\mathrm{B}^0 \to \mathrm{J}/\psi\mathrm{K}^0_\mathrm{S}$, $\mathrm{B}^0_\mathrm{s} \to \mathrm{J}/\psi\pi^+\pi^-$, $\mathrm{B}^0_\mathrm{s} \to \mathrm{J}/\psi\phi(1020)$, $\mathrm{B}^+_\mathrm{c} \to \mathrm{J}/\psi\pi^+$ and $\Lambda^0_\mathrm{b} \to \mathrm{J}/\psi\Lambda^0$, where $\mathrm{K}^*(892)^0 \to \mathrm{K}^+\pi^-$, $\mathrm{K}^0_\mathrm{S} \to \pi^+\pi^-$, $\phi(1020) \to \mathrm{K}^+\mathrm{K}^-$, and $\Lambda^0 \to \mathrm{p}\pi^-$. Charge conjugation is implied.

The decay rate of neutral $\mathrm{B}^0_{(\mathrm{s})}$ mesons is characterised by two parameters, the average decay width $\Gamma_\mathrm{q} = (\Gamma^\mathrm{q}_\mathrm{L} + \Gamma^\mathrm{q}_\mathrm{H})/2$ and the decay width difference $\Delta\Gamma_\mathrm{q} = \Gamma^\mathrm{q}_\mathrm{L} - \Gamma^\mathrm{q}_\mathrm{H}$ defined with the decay widths $\Gamma^\mathrm{q}_{\mathrm{L,H}}$ of the light (L) and heavy (H) mass eigenstates. Assuming no flavour specific asymmetry at the production, the time-dependent decay rate of the neutral B^0_q mesons into a final state f is [3]

$$\Gamma(\mathrm{B}^0_\mathrm{q} \to f) = \Gamma(\mathrm{B}^0_\mathrm{q}) + \Gamma(\overline{\mathrm{B}}^0_\mathrm{q}) = R^f_\mathrm{L} e^{-\Gamma^\mathrm{q}_\mathrm{L} t} + R^f_\mathrm{H} e^{-\Gamma^\mathrm{q}_\mathrm{H} t}, \tag{2}$$

where R^f_L and R^f_H are the amplitudes of light and heavy mass states, respectively. Since the neutral B mesons have two eigenstates with different lifetimes, the ct distribution consists of two exponentials. The average lifetime of neutral B mesons, produced as an equal admixture of B^0_q and $\overline{\mathrm{B}}^0_\mathrm{q}$ flavour eigenstates, is defined as

$$\tau_{\mathrm{B}^0_\mathrm{q} \to f} = \frac{\int_0^\infty t\frac{d\Gamma(t)}{dt}dt}{\int_0^\infty \frac{d\Gamma(t)}{dt}dt} = \frac{\frac{R^f_\mathrm{L}}{\left(\Gamma^\mathrm{q}_\mathrm{L}\right)^2} + \frac{R^f_\mathrm{H}}{\left(\Gamma^\mathrm{q}_\mathrm{H}\right)^2}}{\frac{R^f_\mathrm{L}}{\Gamma^\mathrm{q}_\mathrm{L}} + \frac{R^f_\mathrm{H}}{\Gamma^\mathrm{q}_\mathrm{H}}}. \tag{3}$$

Since the amplitudes R^f_H and R^f_L are specific to the decay channel, the average lifetime depends on the final state f. Lifetimes measured by fitting an exponential function to the distribution consisting of two exponentials are called *effective lifetimes*. In the B^0_s system, $\frac{\Delta\Gamma_\mathrm{s}}{\Gamma_\mathrm{s}} = 12.4 \pm 1.1\%$ [4] and the deviation from an exponential ct distribution is sizeable. Since the B^0 system has a small lifetime difference with respect to the average lifetime, $\frac{\Delta\Gamma_\mathrm{d}}{\Gamma_\mathrm{d}} = -0.3 \pm 1.5\%$ [4], the ct distribution is close to an exponential, and is treated as such for the lifetime measurement.

In this analysis, two lifetimes associated to the B_s^0 meson are measured in the final states of $J/\psi\phi(1020)$ and $J/\psi\pi^+\pi^-$. The $B_s^0 \to J/\psi\pi^+\pi^-$ decays are reconstructed in the invariant mass range $0.9240 < M(\pi^+\pi^-) < 1.0204$ GeV, which is dominated by the $f_0(980)$ resonance [5, 6], making it a CP-odd final state. The lifetime measured in this channel is related to the inverse of the decay width of the heavy B_s^0 mass eigenstate, $\tau_{B_s^0}^{\text{CP-odd}} \approx 1/\Gamma_H$, in the limit of no CP violation in the mixing. The final state $J/\psi\phi(1020)$ is an admixture of two CP-even states and one CP-odd state, corresponding to the light and heavy mass eigenstates, respectively, neglecting CP violation in mixing. The effective lifetime of the B_s^0 meson decaying to $J/\psi\phi(1020)$ can be written as

$$c\tau_{\text{eff}} = \frac{|A|^2(c\tau_L)^2 + |A_\perp|^2(c\tau_H)^2}{|A|^2 c\tau_L + |A_\perp|^2 c\tau_H} = f_H c\tau_H + (1 - f_H)c\tau_L, \tag{4}$$

where $|A|^2 = |A_0(0)|^2 + |A_\parallel(0)|^2$ is the sum of the amplitudes of the two CP-even states, $|A_\perp|^2 = |A_\perp(0)|^2$ is the amplitude of the CP-odd state, and the heavy component fraction is defined as $f_H = |A_\perp|^2 c\tau_H / (|A|^2 c\tau_L + |A_\perp|^2 c\tau_H)$.

By combining the B_s^0 lifetimes obtained from the final states $J/\psi\phi(1020)$ and $J/\psi\pi^+\pi^-$, it is possible to determine the lifetime of the light B_s^0 eigenstate. The results in this paper are complementary to the weak mixing phase analysis in the $B_s^0 \to J/\psi\phi(1020)$ channel [7], which provided CMS measurements of the average decay width Γ_s and the decay width difference $\Delta\Gamma_s$.

The weak decay of the B_c^+ meson can occur through either the b or c quark decaying with the other quark as a spectator or through an annihilation process. As the annihilation process is predicted to contribute 10% of the decay width, lifetime measurements can be used to test the B_c^+ decay model. As the recent lifetime measurements by LHCb [8, 9] are significantly larger than those measured at the Tevatron [10–12], an additional measurement by CMS may help to resolve this discrepancy.

2 The CMS detector

The central feature of the CMS apparatus is a superconducting solenoid of 6 m internal diameter, providing a magnetic field of 3.8 T. Within the solenoid volume are a silicon pixel and strip tracker, a lead tungstate crystal electromagnetic calorimeter, and a brass and scintillator hadron calorimeter, each composed of a barrel and two endcap sections. Forward calorimeters extend the pseudorapidity coverage provided by the barrel and endcap detectors. Muons are measured in gas-ionization detectors embedded in the steel flux-return yoke outside the solenoid.

The main subdetectors used for the present analysis are the silicon tracker and the muon detection system. The silicon tracker measures charged particles within the pseudorapidity range $|\eta| < 2.5$. It consists of 1440 silicon pixel and 15 148 silicon strip detector modules. For nonisolated particles of $1 < p_T < 10$ GeV and $|\eta| < 1.4$, the track resolutions are typically 1.5% in p_T and 25–90 (45–150) μm in the transverse (longitudinal) impact parameter [13].

Muons are measured in the pseudorapidity range $|\eta| < 2.4$, with detection planes made using three technologies: drift tubes, cathode strip chambers, and resistive plate chambers.

The first level trigger (L1), composed of custom hardware processors, uses information from the calorimeters and muon detectors to select events at a rate of around 100 kHz within a time interval of less than 4 μs. The second level, known as the high-level trigger (HLT), consists of a farm of processors running a version of the full event reconstruction software optimized for

fast processing, and reduces the event rate to less than 1 kHz before data storage. At the HLT stage there is full access to the event information, including tracking, and therefore selection criteria similar to those applied offline can be used.

A more detailed description of the CMS detector, together with a definition of the coordinate system used and the relevant kinematic variables, can be found in Ref. [2].

3 Data and Monte Carlo samples

The data used in this analysis were collected in 2012 by the CMS detector at the LHC in proton-proton collisions at a center-of-mass energy of 8 TeV, and correspond to an integrated luminosity of 19.7 fb^{-1}.

Fully simulated Monte Carlo (MC) samples of $B^0 \to J/\psi K^*(892)^0$, $B^0 \to J/\psi K^0_S$, $B^+ \to J/\psi K^+$, $B^0_s \to J/\psi \pi^+\pi^-$, $B^0_s \to J/\psi\phi(1020)$, and $\Lambda^0_b \to J/\psi\Lambda^0$ were produced with PYTHIA (version 6.424 [14]) to simulate the proton-proton collisions, and to perform the parton shower and hadronization processes. The B^+_c MC sample has been produced using the dedicated generator BCVEGPY [15, 16] interfaced with PYTHIA. Particles containing a b and c quark are decayed with the EVTGEN package [17] and final state radiation is included with PHOTOS [18]. Events are passed through the CMS detector simulation based on the GEANT4 package [19], including digitized signals from MC-simulated inelastic pp events to match the amount of multiple production vertices in the data (pileup). Simulated events are processed with the same reconstruction and trigger algorithms as the data.

4 Reconstruction of b hadrons

The data are recorded with a trigger optimised for collecting B hadrons having a J/ψ meson as a decay product. The trigger reconstructs the J/ψ meson from an oppositely charged muon pair using a set of selection criteria for the muons and the J/ψ candidate. The transverse momentum of the J/ψ candidate is required to be greater than 7.9 GeV and both muons must be in the pseudorapidity region $|\eta(\mu)| < 2.2$. The muons are also required to originate from a common vertex with a probability greater than 0.5%. The invariant mass of the dimuon system must lie within 0.15 GeV of the world average J/ψ mass [4]. Finally, the distance of closest approach between the two muons must be less than 0.5 cm.

The offline selection starts from J/ψ candidates that are reconstructed from pairs of oppositely charged muons and identified through the standard CMS muon reconstruction procedure [20]. The offline selection requirements on the dimuon pair replicate the trigger selection. From the sample of collected J/ψ events, candidate b hadrons are reconstructed by combining a J/ψ candidate with track(s) or reconstructed neutral particles, depending on the decay mode. Only tracks that pass the standard CMS quality requirements [21] are used. In the b hadron vertex fit, the dimuon invariant mass is constrained to the world average J/ψ mass [4], and a mass hypothesis is assigned to the charged track(s). Production vertices (PV) are fitted from the reconstructed tracks using the estimate of the proton-proton interaction region (beam spot) as a constraint. The PV having the smallest pointing angle, defined as the angle between the reconstructed b hadron momentum and the vector joining the PV with the decay vertex, is used.

4.1 Reconstruction of B^+, B^0, B_s^0 and Λ_b^0

The B^+, B^0, B_s^0, and Λ_b^0 hadrons are reconstructed in the decays $B^+ \to J/\psi K^+$, $B^0 \to J/\psi K_S^0$, $B^0 \to J/\psi K^*(892)^0$, $B_s^0 \to J/\psi \pi^+\pi^-$, $B_s^0 \to J/\psi\phi(1020)$, and $\Lambda_b^0 \to J/\psi\Lambda^0$. The $K^*(892)^0$, K_S^0, $\phi(1020)$, and Λ^0 candidates are reconstructed from pairs of oppositely charged tracks that are consistent with originating from a common vertex. The mass assignments for the K_S^0 and $\phi(1020)$ decay products are unambiguous. Since two $K^*(892)^0$ candidates can be formed with a single pair of tracks, we select the combination for which the mass of the $K^*(892)^0$ candidate is closest to the world average value [4]. For the kinematic region considered in this analysis, simulations show that the proton always corresponds to the track with the higher momentum (leading track) from the Λ^0 decay. The fit to form the B^0 (Λ_b^0) candidates constrains both the J/ψ and K_S^0 (Λ^0) candidate masses to their world average values [4].

All tracks must have transverse momentum greater than 0.5 GeV. The decay vertices of the K_S^0 and Λ^0 particles are required to have a transverse distance significance larger than 15 and their decay products must have a transverse impact parameter significance of at least 2 with respect to the beam spot. Intermediate reconstructed candidate resonances are selected if they lie within the following mass regions ($\pm$1.3–2 times the experimental resolution or natural width around the nominal mass): $0.7960 < M(K^*(892)^0) < 0.9880$ GeV, $0.4876 < M(K_S^0) < 0.5076$ GeV, $0.9240 < M(\pi^+\pi^-) < 1.0204$ GeV, $1.0095 < M(\phi(1020)) < 1.0295$ GeV and $1.1096 < M(\Lambda^0) < 1.1216$ GeV. The K_S^0 contamination in the Λ^0 sample is removed by discarding events in which the proton from the Λ^0 decay is assumed to be a pion and $0.4876 < M(\pi\pi) < 0.5076$ GeV. Conversely, Λ^0 contamination is removed from the K_S^0 sample by discarding events in the mass region $1.1096 < M(p\pi) < 1.1216$ GeV, where the mass of the leading pion from the K_S^0 decay has been substituted with the proton mass. The p_T of the K^+ candidate track from the B^+ decay must be larger than 1 GeV. The leading (trailing) $K^\pm$ or $\pi^\pm$ candidate track from the $K^*(892)^0$ and $\pi^+\pi^-$ (from the B_s^0) decays are required to have a p_T greater than 2.5 GeV (1.5 GeV). The p_T of the leading track from K_S^0 and Λ^0 decays must be larger than 1.8 GeV. The minimum p_T for the kaons forming a $\phi(1020)$ candidate is 0.7 GeV. The p_T of the $\pi^+\pi^-$ system in $B_s^0 \to J/\psi\pi^+\pi^-$, and $K^*(892)^0$ candidates in $B^0 \to J/\psi K^*(892)^0$ has to be larger than 3.5 GeV. The p_T of the b hadrons must be at least 13 GeV except for the $B_s^0 \to J/\psi\phi(1020)$ decay where no requirement is imposed. The b hadron χ^2 vertex probability is required to be greater than 0.1% only in the $B_s^0 \to J/\psi\phi(1020)$ channel. The lifetime measurement is limited to events in which the b hadron ct is greater than 0.02 cm.

4.2 Reconstruction of $B_c^+ \to J/\psi\pi^+$

The B_c^+ lifetime is measured using the method developed by LHCb [9] in which the measured difference in total widths between the B_c^+ and B^+ mesons is used in combination with the precisely known B^+ lifetime to obtain the B_c^+ lifetime. The same reconstruction algorithm and selection criteria are used for both decays, $B_c^+ \to J/\psi\pi^+$ and $B^+ \to J/\psi K^+$. As a result, the efficiencies as a function of the proper decay time are similar.

The reconstructed charged hadrons are required to have at least 6 tracker hits, at least 2 pixel hits, a track fit χ^2 less than 3 times the number of degrees of freedom, and $|\eta| < 2.4$. The dimuon invariant mass is required to lie in the range $\pm 3\sigma$ from the nominal J/ψ mass, where σ is the average resolution of the J/ψ signal, which depends on the J/ψ pseudorapidity. The p_T of the charged hadron tracks and the b hadrons are required to be greater than 3.3 GeV and 10 GeV, respectively. The b hadrons must have rapidity of $|y| < 2.2$, a vertex χ^2 probability greater than 5%, a dimuon vertex χ^2 probability greater than 1%, and $\cos\theta > 0.98$, where $\cos\theta = L_{xy} \cdot p_{T,B}/(|L_{xy}| \cdot |p_{T,B}|)$ and the quantities L_{xy} and $p_{T,B}$ refer to the transverse decay

length and momentum of the B^+ and B_c^+. The lifetime measurement is limited to events in which the b hadron has $ct > 0.01\,\text{cm}$, which is the minimum requirement that ensures a constant value versus ct for the ratio of B_c^+ to B^+ efficiencies.

5 Data modelling and fit results

For each b hadron we perform a three dimensional unbinned maximum likelihood (ML) fit to the data. The distributions that are simultaneously fit are the b hadron mass, ct, and per-event ct uncertainty. The efficiency correction is incorporated into the fit by multiplying an exponential probability density function (PDF) describing the b hadron ct distribution with the efficiency parametrisation. The parameters of the efficiency function and the functions modelling the ct uncertainty distribution are kept constant in the ML fit for each of the fit models. The other fit parameters can vary freely.

5.1 Data modelling

Depending on the decay channel, the invariant mass distribution for the signal is modelled with one or two Gaussian functions, and a linear polynomial or an exponential function is used to model the combinatorial background. For the $B_s^0 \to J/\psi\pi^+\pi^-$ decay, additional terms are added to include backgrounds from partially reconstructed or misidentified b hadron decays. Backgrounds from decays such as $B^0_{(d,s)} \to J/\psi + h_1^+ h_2^-$ are modelled by a Gaussian function below the B_s^0 mass peak, and for $B^+ \to J/\psi K^+$ decays the shape is taken from simulation.

For the ct distribution, the signal is modelled by an exponential decay convolved with the detector resolution, which is assumed to be a Gaussian with the width defined by the calculated uncertainty on ct. The backgrounds are described by a superposition of exponential functions convolved with the resolution. The number of exponentials depends on the decay channel and is determined using events in the mass sideband regions.

The signal and background σ_{ct} distributions are modelled with either a sum of two gamma functions or two exponential functions convolved with a Gaussian function. The parameters of the functions are obtained from the sideband subtracted fit to the data for the signal and from events in the mass sideband regions for the background.

The measurement of the B_s^0 lifetime in both decay modes is performed with an unbinned *extended* maximum likelihood fit (EMLF). In the $B_s^0 \to J/\psi\pi^+\pi^-$ fit, the background model parameters are allowed to float in the EMLF, except for the parameters describing the B^+ mass shape, which are taken from the simulation. However, the yield and the lifetime of the $B^+ \to J/\psi K^+$ decays contaminating the B_s^0 sample are free parameters of the fit.

5.2 Efficiency

For each decay channel, the efficiency is determined as a function of ct by using fully simulated MC samples. The efficiency is defined as the generated ct distribution of the selected events after reconstruction divided by the ct distribution obtained from an exponential decay with the lifetime set to the value used to generate the events. The efficiency for the $B_s^0 \to J/\psi\phi(1020)$ channel is defined as the generated ct distribution of the selected events after reconstruction divided by the sum of the two exponentials generated with the theoretical $B_s^0 \to J/\psi\phi(1020)$ decay rate model. In the theoretical model, the values of the physics parameters are set to those used in the simulated sample.

Figure 1 shows the efficiency for the various decay modes. In all cases, the efficiency has a

turn-on shape for *ct* values lower than 0.02 cm. Above this value, the efficiency exhibits a slow decrease. The *ct* efficiency is modelled with a inverse power function.

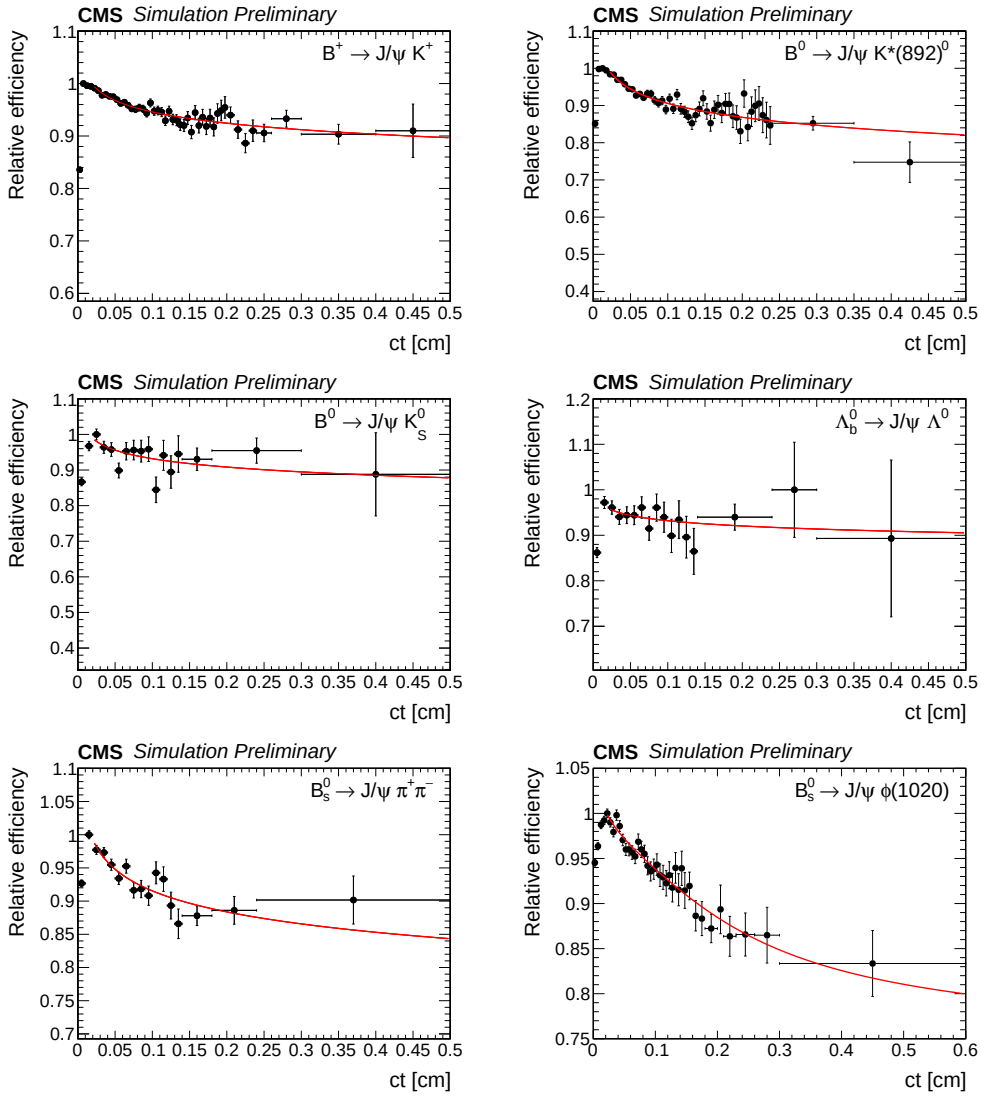

Figure 1: Efficiency versus *ct* with a superimposed fit to a inverse power function for B^+ (top left), $B^0 \to J/\psi K^*(892)^0$ (top right), $B^0 \to J/\psi K^0_S$ (center left), Λ^0_b (center right), $B^0_s \to J/\psi\pi^+\pi^-$ (bottom left), and $B^0_s \to J/\psi\phi(1020)$ (bottom right). The efficiency scale is arbitrary.

5.3 Fit results

The invariant mass and *ct* distributions obtained from data are shown with the fit results superimposed in Figs. 2–7. The *ct* distribution is fit in the range of 0.02–0.50 cm for all modes except the $B^0_s \to J/\psi\phi(1020)$ channel, where the upper limit is increased to 0.60 cm. The average lifetimes obtained from the fits are: $c\tau_{B^+} = 490.9 \pm 0.8\ \mu$m, $c\tau_{B^0 \to J/\psi K^*(892)^0} = 453.0 \pm 1.6\ \mu$m, $c\tau_{B^0 \to J/\psi K^0_S} = 457.8 \pm 2.7\ \mu$m, $c\tau_{B^0_s \to J/\psi\pi^+\pi^-} = 504.3 \pm 10.5\ \mu$m, $c\tau_{B^0_s \to J/\psi\phi(1020)} = 445.2 \pm 2.0\ \mu$m and $c\tau_{\Lambda^0_b} = 443.1 \pm 8.2\ \mu$m, where all uncertainties are statistical only. Neglecting CP violation in mixing, the measured $B^0_s \to J/\psi\pi^+\pi^-$ lifetime can be translated into the width of the heavy B^0_s mass eigenstate $\Gamma_H = 0.594 \pm 0.012\ \text{ps}^{-1}$.

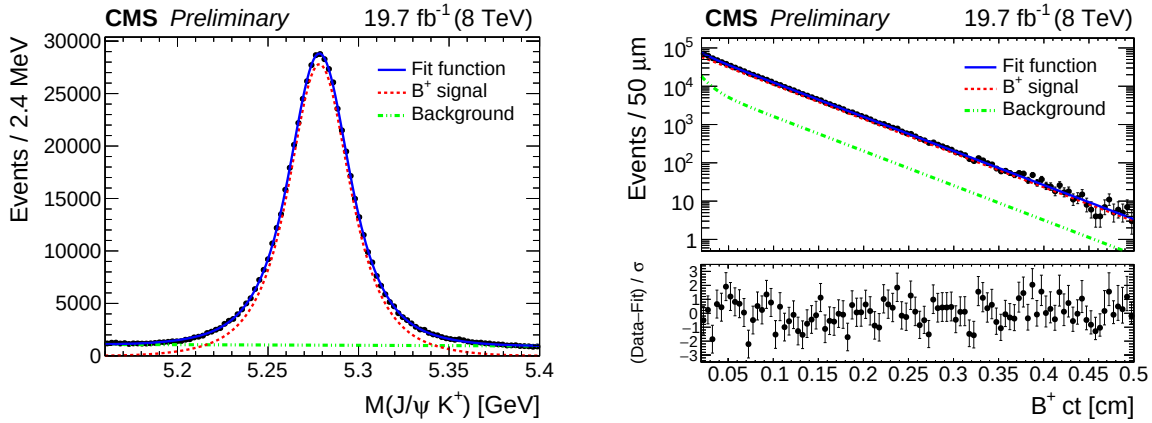

Figure 2: Invariant mass (left) and *ct* (right) distributions for B^+ candidates. The curves are projections of the maximum-likelihood fit to the data, with the contributions from signal (dashed), background (dotted), and the sum of signal and background (solid) shown. The bottom panel of the right figure shows the difference between the observed data and the fit divided by the data uncertainty.

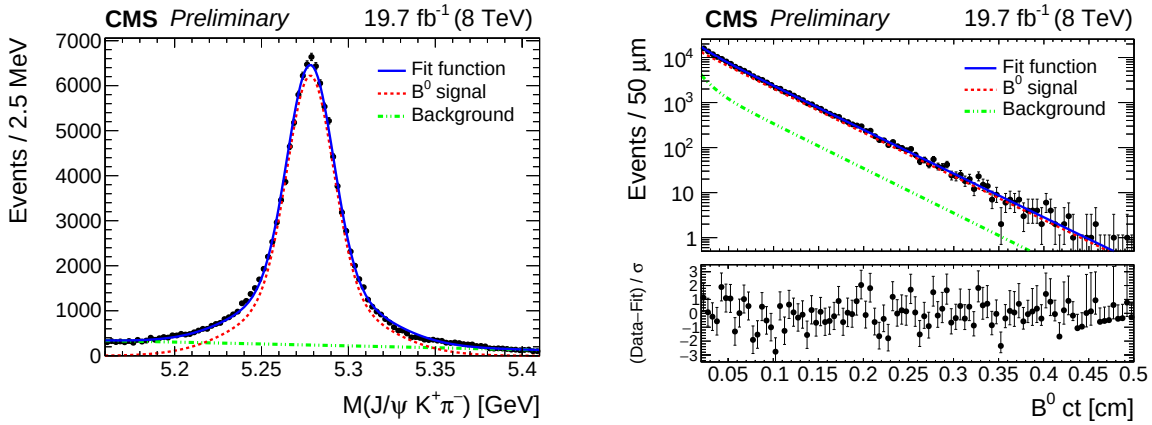

Figure 3: Invariant mass (left) and *ct* (right) distributions for B^0 candidates reconstructed from $J/\psi K^*(892)^0$ decays. The curves are projections of the maximum-likelihood fit to the data, with the contributions from signal (dashed), background (dotted), and the sum of signal and background (solid) shown. The bottom panel of the right figure shows the difference between the observed data and the fit divided by the data uncertainty.

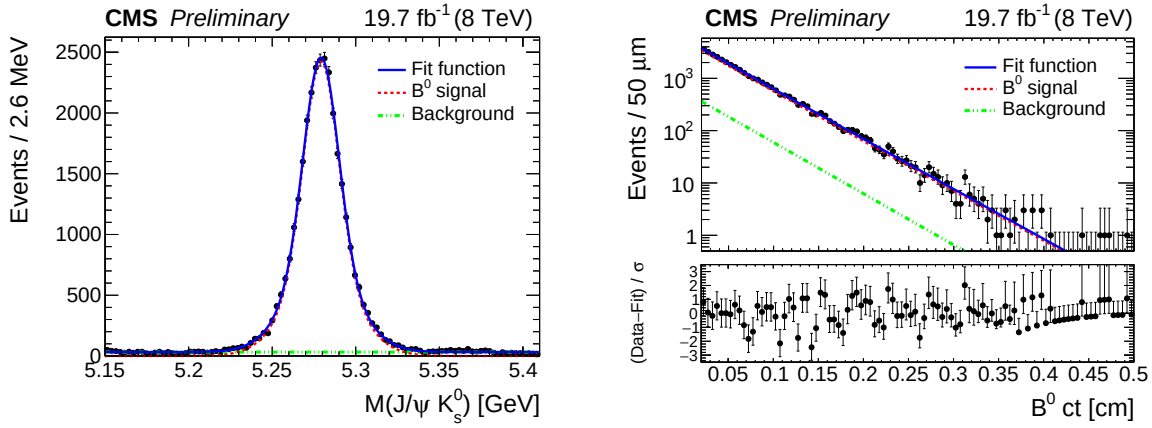

Figure 4: Invariant mass (left) and *ct* (right) distributions for B^0 candidates reconstructed from $J/\psi K^0_S$ decays. The curves are projections of the maximum-likelihood fit to the data, with the contributions from signal (dashed), background (dotted), and the sum of signal and background (solid) shown. The bottom panel of the right figure shows the difference between the observed data and the fit divided by the data uncertainty.

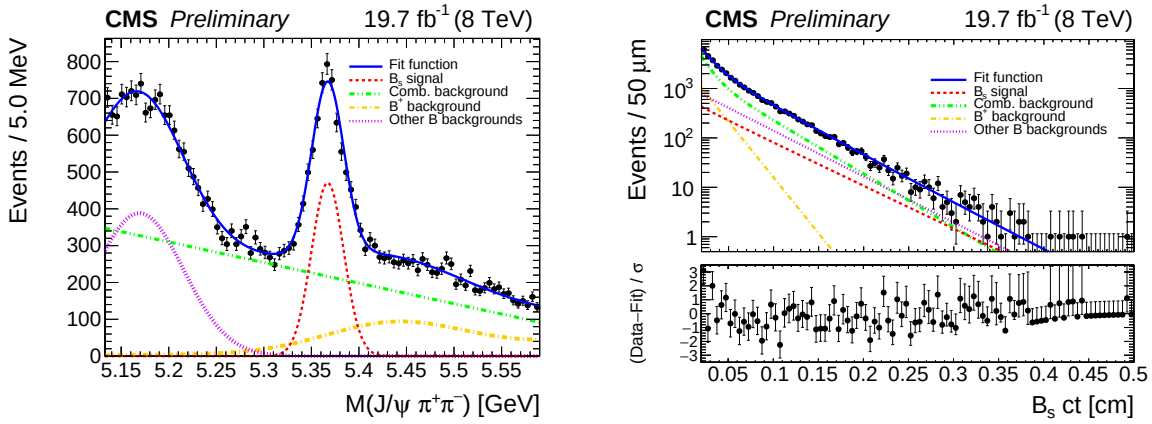

Figure 5: Invariant mass (left) and *ct* (right) distributions for B^0_s candidates reconstructed from $J/\psi\pi^+\pi^-$ decays. The curves are projections of the maximum-likelihood fit to the data, with the contributions from signal (dashed), combinatorial background (dotted), misidentified $B^+ \to J/\psi K^+$ background (dashed-dotted), partially reconstructed and (other) misidentified B backgrounds (vertical dashed), and the sum of signal and backgrounds (solid) shown. The bottom panel of the right figure shows the difference between the observed data and the fit divided by the data uncertainty.

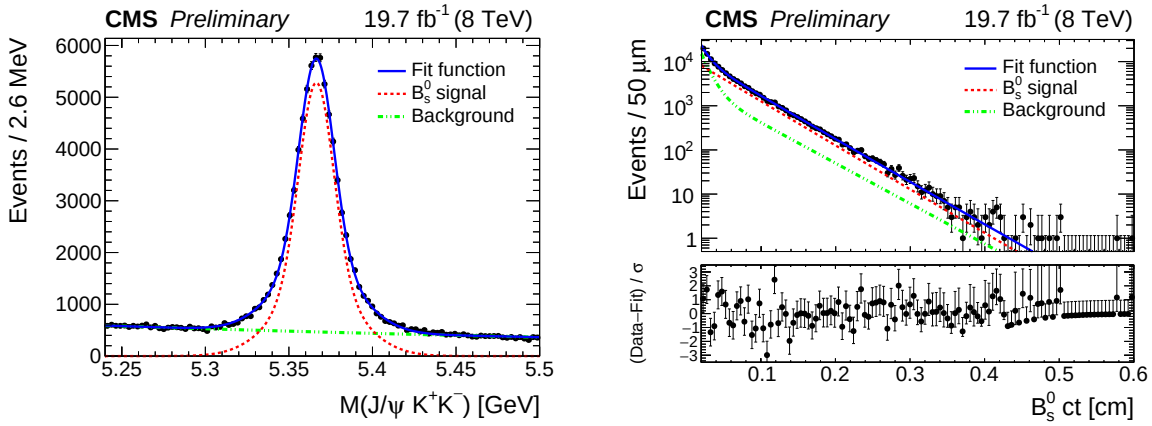

Figure 6: Invariant mass (left) and *ct* (right) distributions for B_s^0 candidates reconstructed from $J/\psi\phi(1020)$ decays. The curves are projections of the maximum-likelihood fit to the data, with the contributions from signal (dashed), background (dotted), and the sum of signal and background (solid) shown. The bottom panel of the right figure shows the difference between the observed data and the fit divided by the data uncertainty.

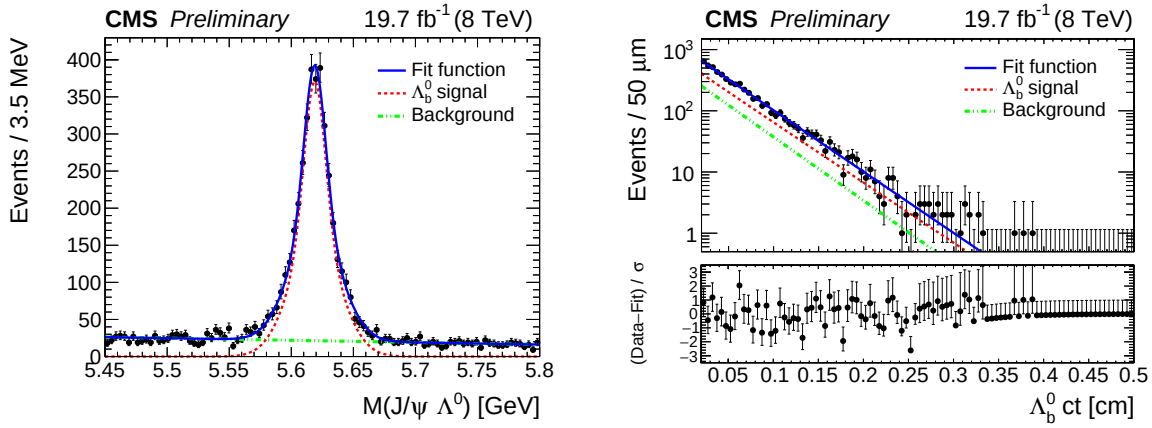

Figure 7: Invariant mass (left) and *ct* (right) distributions for Λ_b^0 candidates. The curves are projections of the maximum-likelihood fit to the data, with the contributions from signal (dashed), background (dotted), and the sum of signal and background (solid) shown.The bottom panel of the right figure shows the difference between the observed data and the fit divided by the data uncertainty.

6 Systematic uncertainties

Systematic uncertainties can be divided into uncertainties common to all the measurements, and uncertainties specific to a decay channel. Table 1 summarizes the systematic uncertainties for the sources considered below and the total systematic uncertainty.

We verified that results are stable under different selection requirements on the quality of the tracks and vertices, kinematics, ct, as well as in several detector regions and data taking epochs. The effect of replacing the mass of the b hadron in the ct definition from the world average to to the reconstructed mass is found to be negligible.

6.1 Common systematic uncertainties

1. Production vertex selection

   The data contain multiple primary vertices generated in each of the beam crossings from which one is selected to compute ct. Different options to select the PV were studied for the case of the B^+ lifetime, the sample with the smallest statistical uncertainty. While all methods are found to be effective and unbiased, there were small differences and the maximum deviation with respect to the nominal choice is taken as the systematic uncertainty.

2. Detector alignment

   Possible effects on the lifetime due to the uncertainties in the detector alignment are investigated in different simulated samples with distorted geometries for each decay topology. The average dispersion (standard deviation) of the lifetimes for the tested scenarios is taken as the systematic uncertainty from this source.

3. ct resolution

   The calculated resolution σ_{ct} is multiplied by a scale factor s to account for a possible bias in the calculation. For each b hadron, the lifetime fit is repeated with $s = 0.5$ and $s = 2.0$ and the maximum variation with respect to the nominal lifetime measurement is taken as the systematic uncertainty.

4. MC finite size

   The number of events in the simulation directly affects the accuracy of the efficiency determination. To propagate this uncertainty to the measured lifetime, 1000 efficiency curves are generated with variations of the parameter values. The parameter values are sampled using a multivariate Gaussian probability density function that is constructed from the covariance matrix of the efficiency fit. The analysis is run 1000 times with varying parameters of the efficiency function. The distribution of the measured lifetimes is fitted with a Gaussian, whose width is taken as the systematic uncertainty associated with the finite size of the simulated samples.

5. Efficiency modelling

   In addition to the efficiency functions used in the nominal fit models, the efficiencies in each decay channel are parametrised with two alternative functions. The new models are fit to the data and the maximum difference of the fit results with respect to the nominal result is taken as a systematic uncertainty.

6. Absolute ct accuracy

The lifetime of the most statistically precise mode ($B^+ \to J/\psi K^+$) is used to validate the absolute ct accuracy. The difference between the measured lifetime and the world average [4] is taken as the systematic uncertainty related to the absolute ct accuracy.

7. Modelling of the mass distribution shape

   Biases related to the shapes of the signal and background probability density functions of the b hadron mass model are quantified by changing the signal and background PDFs individually and using the new models to fit the data. For the background model we use a higher degree polynomial, Chebychev polynomial, or switch from a polynomial function to an exponential. Instead of two Gaussian functions, a single Gaussian function or a sum of three Gaussian functions is used to model the signal mass peak. The difference between the results of the nominal and alternative model is quoted as the systematic uncertainty. Lifetime variations due to the modelling of signal and background components are evaluated separately and added in quadrature to form a systematic uncertainty for the mass modelling.

8. Modelling of the background ct shape

   To estimate a systematic uncertainty due to the ct background model, we increase the number of exponential functions with respect to those used in the nominal fit models. The difference between the results of the nominal and alternative fit model is used as the systematic uncertainty from the ct shape modelling.

6.2 Channel specific systematic uncertainties

1. B^+ contamination in the $B_s^0 \to J/\psi\pi^+\pi^-$ sample

   An alternative estimate of the $J/\psi K^+$ contamination is obtained from data by taking the leading pion of the $B_s^0 \to J/\psi\pi^+\pi^-$ decay to be the kaon. The effective lifetime and yield of the $B^+ \to J/\psi K^+$ decays contaminating the $B_s^0 \to J/\psi\pi^+\pi^-$ sample are determined from a fit of the B^+ signal candidates in the $B_s^0 \to J/\psi\pi^+\pi^-$ sample and the mass shape is also obtained from the data. The B_s^0 lifetime found with this model is considered as the systematic uncertainty due to B^+ contamination.

2. Invariant mass window of the $\pi^+\pi^-$ in the $B_s^0 \to J/\psi\pi^+\pi^-$ channel

   Although the events selected by the $\pi^+\pi^-$ mass window are dominated by the $f_0(980)$, its width is not well known and possible backgrounds under the $f_0(980)$ peak could be increased or reduced, depending on the mass window. The effect on the lifetime is studied by using mass windows of ± 30 and 80 MeV around the signal peak, compared to the nominal fit result with a ± 50 MeV window. The maximum variation of the lifetime is taken as the systematic uncertainty.

3. $K^\pm\pi^\mp$ mass assumption for $K^*(892)^0$ candidates in the $B^0 \to J/\psi K^*(892)^0$ channel

   The $K^*(892)^0$ candidates are constructed from a pair of tracks with kaon and pion mass assignments. Due to the lack of charged particle identification, there are two possible combinations. The combination with invariant mass closest to the world average $K^*(892)^0$ mass is chosen to reconstruct the B^0 candidate. To estimate the effect on the lifetime due to a possible misassignment of kaon and pion, both combinations are discarded if both are within the natural width of the $K^*(892)^0$ mass, and the difference between the lifetime obtained with this sample and the nominal sample is taken as the systematic uncertainty.

4. The ct range in $B_s^0 \to J/\psi\phi(1020)$ channel

   Since the $ct > 200\,\mu$m requirement distorts the fractions of heavy and light mass eigenstates, the measured effective lifetime must be corrected. The correction and systematic uncertainty are quantified analytically.

   The correction to the effective lifetime is defined as

$$\delta_{ct} = c\tau_{\text{eff}}^{\text{cut}} - c\tau_{\text{eff}} = \frac{|A|^2(c\tau_L)^2 e^{-a/c\tau_L} + |A_\perp|^2(c\tau_H)^2 e^{-a/c\tau_H}}{|A|^2 c\tau_L e^{-a/c\tau_L} + |A_\perp|^2 c\tau_H e^{-a/c\tau_H}} - \frac{|A|^2(c\tau_L)^2 + |A_\perp|^2(c\tau_H)^2}{|A|^2 c\tau_L + |A_\perp|^2 c\tau_H}, \tag{5}$$

   where the first term represents the effective lifetime in the presence of a $ct > a$ requirement and the latter term is the unbiased effective lifetime. In this analysis a is equal to 200 μm.

   The world average values [4] for $c\tau_H = 482.7 \pm 3.6\,\mu$m, $c\tau_L = 426.3 \pm 2.4\,\mu$m, and $|A_\perp|^2 = 0.250 \pm 0.006$ are used to obtain the correction and uncertainty of $\delta_{ct} = 0.62 \pm 0.10\,\mu$m.

5. S-wave contamination in the $B_s^0 \to J/\psi\phi(1020)$ channel

   The B_s^0 candidates reconstructed in the $J/\psi\phi(1020)$ final state contain a small fraction of non-resonant and CP-odd $B_s^0 \to J/\psi K^+K^-$ decay where the invariant mass of the two kaons is consistent with the ϕ meson mass.

   The fraction of $B_s^0 \to J/\psi K^+K^-$ decays among the selected events is measured in the weak mixing phase analysis [7] to be $f_S = 1.2^{+0.9}_{-0.7}\%$. Due to the different trigger and signal selection criteria of the present analysis, the S-wave fraction is corrected according to the simulation to be $1.5^{+1.1}_{-0.9}\%$.

   The bias caused by the contamination of nonresonant $B_s^0 \to J/\psi K^+K^-$ decays is estimated by generating two sets of pseudo-experiments, one with just $B_s^0 \to J/\psi\phi(1020)$ events and one with a fraction of S-wave events based on the measured S-wave fraction and its uncertainty. The difference in the average of the measured lifetimes of these two samples is 0.74 μm, which is used to correct the measured lifetime. The systematic uncertainty associated with this correction is obtained by taking the difference in quadrature between the standard deviation of the distribution of lifetime results from the pseudo-experiments with and without the S-wave contribution.

7 Measurement of the B_c^+ lifetime

The decay time distribution for the signal $N_B(t)$ can be expressed as the product of an efficiency function $\epsilon_B(t)$ and an exponential decay function $E_B(t) = \exp(-t/\tau_B)$ convolved with the time resolution of the detector $r(t)$. The ratio $N_{B_c^+}(t)/N_{B^+}(t)$, i.e, the ratio of B_c^+ and B^+ events at a given proper time, can be expressed as

$$\frac{N_{B_c^+}(t)}{N_{B^+}(t)} = \mathcal{R}(t) = \frac{\epsilon_{B_c^+}(t) r(t) \otimes E_{B_c^+}(t)}{\epsilon_{B^+}(t) r(t) \otimes E_{B^+}(t)}. \tag{6}$$

Studies have verified that Eq. (6) is not significantly affected by the time resolution, and therefore this equation can be simplified to

$$\mathcal{R}(t) = R_\epsilon(t) \exp(-\Delta\Gamma t), \tag{7}$$

Source	Decay channel				
	$B^0 \to J/\psi K^*(892)^0$	$B^0 \to J/\psi K^0_S$	$B^0_s \to J/\psi \pi^+\pi^-$	$\Lambda^0_b \to J/\psi \Lambda^0$	$B^0_s \to J/\psi \phi$
PV selection	0.7	0.7	0.7	0.7	0.7
Detector alignment	0.3	0.7	0.3	0.7	0.3
ct resolution	0.0	0.1	0.1	0.2	0.1
MC finite size	1.1	2.4	2.0	2.3	0.6
Efficiency modelling	0.3	0.5	0.6	0.6	0.2
Absolute *ct* accuracy	0.2	0.2	0.2	0.2	0.2
Mass modelling	0.3	0.4	0.5	0.9	0.0
ct modelling	0.1	0.1	0.4	0.1	0.4
B^+ contamination	–	–	2.4	–	–
Mass window of the $\pi^+\pi^-$	–	–	1.5	–	–
$K^\pm\pi^\mp$ mass assumption	0.3	–	–	–	–
ct range	–	–	–	–	0.1
S-wave contamination	–	–	–	–	0.4
Total	1.5	2.7	3.7	2.7	1.2

Table 1: Summary of the systematic uncertainties on the lifetime measurements (in μm). The total systematic uncertainty is the sum in quadrature of all systematic sources.

where the small effect of the time resolution is included in $R_\epsilon(t)$, which denotes the ratio of the efficiency functions, evaluated from MC simulations. The quantity $\Delta\Gamma$ is defined as

$$\Delta\Gamma \equiv \Gamma_{B_c^+} - \Gamma_{B^+} = \frac{1}{\tau_{B_c^+}} - \frac{1}{\tau_{B^+}}, \tag{8}$$

where τ_{B^+} is fixed to the world average value [4].

The $B_c^+ \to J/\psi\pi^+$ and the $B^+ \to J/\psi K^+$ invariant mass distributions, shown in Fig. 8, are each fit with an unbinned maximum likelihood estimator. The $J/\psi\pi^+$ invariant mass distribution is fitted with a Gaussian function for the B_c^+ signal and an exponential function for the background. An additional background contribution from $B_c^+ \to J/\psi K^+$ decays is modeled from a simulated sample of $B_c^+ \to J/\psi K^+$ events and its contribution is constrained using the value of the branching fraction relative to $J/\psi\pi^+$ [22]. The $B_c^+ \to J/\psi\pi^+$ signal yield is 1128 ± 60. The B^+ invariant mass distribution is fit with a sum of two Gaussian distributions with a common mean for the signal and a second-order Chebychev polynomial for the background. Additional contributions from partially reconstructed B^0 and B^+ decays are parametrized with functions determined from $B^+ \to J/\psi\pi^+$ and inclusive $B^0 \to J/\psi X$ MC samples.

7.1 The fit model and results

The B_c^+ lifetime is extracted through a binned chi-square fit to the ratio of the efficiency-corrected *ct* distributions of the $B_c^+ \to J/\psi\pi^+$ and $B^+ \to J/\psi K^+$ channels. The *ct* distribution of B_c^+ and B^+ signals from data is obtained by dividing the data sample in *ct* bins and performing an unbinned maximum likelihood fit to the $J/\psi\pi^+$ and $J/\psi K^+$ invariant mass distribution in each bin, with the peak position and resolution fixed to the values obtained by the fits to the full samples. Varied *ct* bin widths are used to ensure a similar statistical uncertainty on the B_c^+ signal yield among the bins. The binning edges are defined by requiring a relative statistical uncertainty of 12% in each bin. The same binning scheme is used for the B^+ *ct* distribution. The B_c^+ and B^+ yields are shown versus *ct* in the left plot of Fig. 9, where the number of signal events is normalized to the bin width. The efficiency is evaluated on the MC samples and is defined

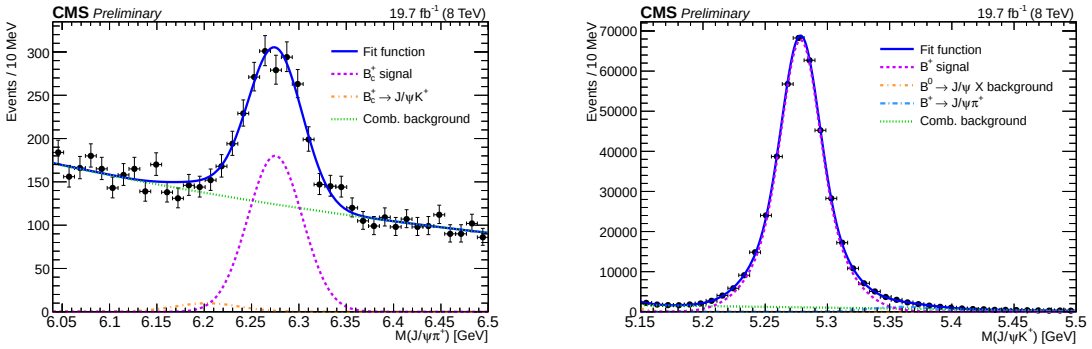

Figure 8: The $J/\psi\pi^+$ invariant mass distribution (left). The solid line represents the signal-plus-background fit. The dashed line represents the signal component, the dotted line the combinatorial background, and the dashed-dotted line the contribution from $B_c^+ \to J/\psi K^+$ decays. The $J/\psi K^+$ invariant mass distribution (right). The result of the fit is superimposed with a solid line. The signal is shown with a dashed line, the dotted-dashed curves represent the $B^+ \to J/\psi\pi^+$ and B^0 contributions, and the dotted curve the combinatorial background.

as the ct distribution of the selected events after reconstruction divided by the ct distribution obtained from an exponential decay with the lifetime set to the same value used to generate each MC sample. The ratio of the two efficiency distributions, using the same binning scheme as in data, is shown in the right plot of Fig. 9.

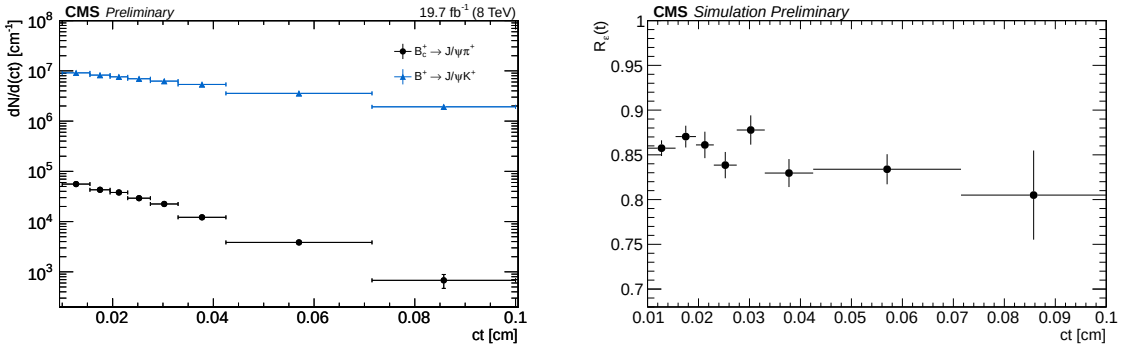

Figure 9: The yield (left) of $B_c^+ \to J/\psi\pi^+$ and $B^+ \to J/\psi K^+$ events as a function of ct, normalized to the bin width, as determined from fits to the invariant mass distributions. Ratio (right) of the B_c^+ and B^+ efficiency distributions as a function of ct.

The ratio of the efficiency-corrected ct distributions from data is shown in Fig. 10, along with the result of a fit to an exponential function. The fit returns $\Delta\Gamma = 4.12 \pm 0.30\ c/\text{mm}$. Using the known lifetime of the B^+meson, $\tau_{B^+} = 1.638 \pm 0.004$ ps [4], a measurement of the B_c^+ meson lifetime, $162.3 \pm 8.2\ \mu$m, is extracted.

7.2 Systematic uncertainties

Various sources of systematic uncertainties on the measurement of $\Delta\Gamma$ are considered; the dominant uncertainty results from the signal and background modeling.

1. Production vertex selection

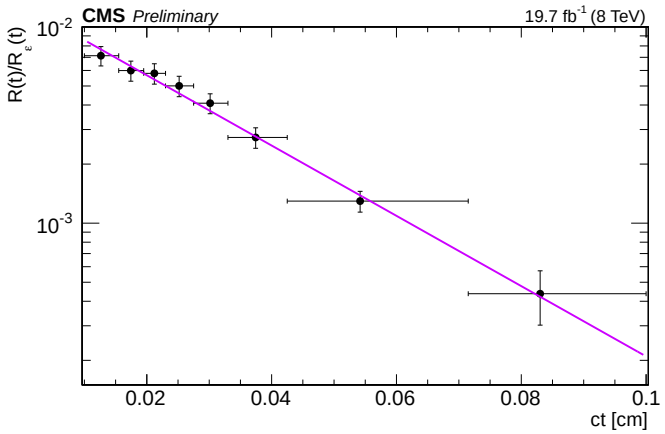

Figure 10: Ratio of the efficiency-corrected ct distributions for B_c^+ and B^+ signals. The line shows the result of fitting with an exponential function.

A possible systematic uncertainty arising from the selection of the primary vertex is evaluated by testing alternative choices and using the maximum deviation with respect to the nominal choice as the systematic uncertainty.

2. Fit model uncertainty

   The fit model uncertainty is accounted for by using different signal and background models to fit the B_c^+ signal in data. The B_c^+ signal peak is alternatively modeled with a Crystal Ball [23, 24] distribution. The alternative description for the background is a Chebychev first order polynomial distribution. The removal of the Cabibbo-suppressed $B_c^+ \to J/\psi K^+$ mode parametrization is also considered. The maximum deviation of the signal yield in each ct bin from the nominal value is propagated to the statistical uncertainty of the per-bin yield. The fit to $R(t)$ is performed and the difference in quadrature between the uncertainty from this fit and from the nominal measurement is considered as the systematic uncertainty.

3. Binning definition

   Different ct binning schemes are tested, requiring a statistical uncertainty on the B_c^+ signal yield of 10%, 15%, and 20%. The systematic uncertainty arising from the choice of the binning has been evaluated using a "fit variant" approach [25].

4. Number of events in the simulated samples

   The bin-by-bin statistical uncertainty on the efficiency determination is propagated to the $R(t)$ distribution, the fit is performed and the difference in quadrature of the uncertainty on $\Delta\Gamma$ with respect to the nominal value is taken as the systematic uncertainty.

5. Detector alignment

   Possible effects on the lifetime measurement due to uncertainties in the detector alignment are evaluated performing the lifetime measurement on simulated samples with distorted geometries. The standard deviation of the results is taken as the systematic uncertainty.

By adding in quadrature the various sources of uncertainty, summarized in Table 2, a total systematic uncertainty of 0.16 c/mm is obtained. Using the known lifetime of the B^+ meson,

this is converted into a systematic uncertainty on the B_c^+ lifetime measurement of 4.7 μm. The uncertainty on the B_c^+ lifetime due to the uncertainty on the B^+ meson lifetime [4] is quoted separately in the result.

Source	$\sigma_{\Delta\Gamma}$ [c/mm]	$\sigma_{c\tau_{B_c^+}}$ [μm]
PV choice	0.07	2.0
Fit model	0.12	3.7
ct binning	0.06	1.6
Simulation size	0.04	1.3
Misalignment	0.03	0.6
Total uncertainty	0.16	4.7

Table 2: Summary of the systematic uncertainties on the $\Delta\Gamma$ and $\tau_{B_c^+}$ measurements.

8 Lifetime measurement results

The lifetimes of the B^0, B_s^0 and Λ_b^0 hadrons reconstructed from the decays $B^0 \to J/\psi K^*(892)^0$, $B^0 \to J/\psi K_S^0$, $B_s^0 \to J/\psi\pi^+\pi^-$, $B_s^0 \to J/\psi\phi(1020)$ and $\Lambda_b^0 \to J/\psi\Lambda^0$ have been measured to be:

$$c\tau_{B^0} = 453.0 \pm 1.6\ (\text{stat}) \pm 1.5\ (\text{syst})\ \mu\text{m}\ (\text{in } J/\psi K^*(892)^0), \quad (9)$$

$$c\tau_{B^0} = 457.8 \pm 2.7\ (\text{stat}) \pm 2.7\ (\text{syst})\ \mu\text{m}\ (\text{in } J/\psi K_S^0), \quad (10)$$

$$c\tau_{B_s^0} = 504.3 \pm 10.5\ (\text{stat}) \pm 3.7\ (\text{syst})\ \mu\text{m}\ (\text{in } J/\psi\pi^+\pi^-), \quad (11)$$

$$c\tau_{B_s^0} = 443.9 \pm 2.0\ (\text{stat}) \pm 1.2\ (\text{syst})\ \mu\text{m}\ (\text{in } J/\psi\phi(1020)), \quad (12)$$

$$c\tau_{\Lambda_b^0} = 443.1 \pm 8.2\ (\text{stat}) \pm 2.7\ (\text{syst})\ \mu\text{m}. \quad (13)$$

Neglecting CP violation in mixing, the measured $B_s^0 \to J/\psi\pi^+\pi^-$ lifetime can be translated into the width of the heavy B_s^0 mass eigenstate:

$$\Gamma_H = c/c\tau_{B_s^0} = 0.594 \pm 0.012\ (\text{stat}) \pm 0.004\ (\text{syst})\ \text{ps}^{-1}. \quad (14)$$

Solving for $c\tau_L$ from Eq. (4) and using the $B_s^0 \to J/\psi\pi^+\pi^-$ result in Eq. (11), the measured B_s^0 effective lifetime in Eq. (12), and the magnitude squared of the CP-odd amplitude from the PDG, the lifetime of the light component is found to be 419.7 ± 6.4 μm, which is within one standard deviation from the world average value. The uncertainty takes into account the statistical and systematic uncertainties of the measured lifetimes in $B_s^0 \to J/\psi\pi^+\pi^-$ and $B_s^0 \to J/\psi\phi(1020)$ modes.

The measured lifetimes for the B^0 meson in the two different channels are in agreement. In general, all results are in agreement with the world average values [4] and some are at the precision of the world average of these parameters.

The B_c^+ lifetime has been measured using the $B_c^+ \to J/\psi\pi^+$ channel and found to be:

$$c\tau_{B_c^+} = 162.3 \pm 8.2\ (\text{stat}) \pm 4.7\ (\text{syst}) \pm 0.1\ (\tau_{B^+})\ \mu\text{m}, \quad (15)$$

where the systematic uncertainty from the B^+ lifetime uncertainty [4] is quoted separately in the result. This measurement confirms a B_c^+ lifetime value higher than that measured at the Tevatron [10–12] and in agreement with the more recent LHCb measurements [8, 9].

9 Summary

The lifetime measurements of the B^0, B_s^0, B_c^+, and Λ_b^0 hadrons, exploiting the decay channels $B^0 \to J/\psi K^*(892)^0$, $B^0 \to J/\psi K_S^0$, $B_s^0 \to J/\psi\pi^+\pi^-$, $B_s^0 \to J/\psi\phi(1020)$, $\Lambda_b^0 \to J/\psi\Lambda^0$, and $B_c^+ \to J/\psi\pi^+$, have been presented, using proton proton collision events collected by the CMS detector at a centre-of-mass energy of 8 TeV, corresponding to an integrated luminosity of $19.7\,\text{fb}^{-1}$. All measurements are in agreement with the world average values and some are at the precision of the world average of these parameters.

References

[1] CMS Collaboration, "Prompt and non-prompt J/ψ production in pp collisions at $\sqrt{s} = 7$ TeV", *Eur. Phys. J. C* **71** (2011) 1575, doi:10.1140/epjc/s10052-011-1575-8, arXiv:1011.4193.

[2] CMS Collaboration, "The CMS experiment at the CERN LHC", *JINST* **3** (2008) S08004, doi:10.1088/1748-0221/3/08/S08004.

[3] R. Fleischer and R. Knegjens, "Effective lifetimes of B_s decays and their constraints on the B_s^0-$\bar{B}_s^0$ mixing parameters", *Eur. Phys. J. C* **71** (2011) 1789, doi:10.1140/epjc/s10052-011-1789-9, arXiv:1109.5115.

[4] Particle Data Group, C. Patrignani et al., "Review of particle physics", *Chin. Phys. C* **40** (2016) 100001, doi:10.1088/1674-1137/40/10/100001.

[5] LHCb Collaboration, "Analysis of the resonant components in $\bar{B}_s^0 \to J/\psi\pi^+\pi^-$", *Phys. Rev. D* **86** (2012) 052006, doi:10.1103/PhysRevD.86.052006, arXiv:1301.5347.

[6] LHCb Collaboration, "Measurement of resonant and CP components in $\bar{B}_s^0 \to J/\psi\pi^+\pi^-$", *Phys. Rev. D* **89** (2014) 092006, doi:10.1103/PhysRevD.89.092006, arXiv:1402.6248.

[7] CMS Collaboration, "Measurement of the CP-violating weak phase ϕ_s and the decay width difference $\Delta\Gamma_s$ using the $B_s^0 \to J/\psi\phi(1020)$ decay channel in pp collisions at $\sqrt{s} = 8$ TeV", *Phys. Lett. B* **757** (2016) 97, doi:10.1016/j.physletb.2016.03.046, arXiv:1507.07527.

[8] LHCb Collaboration, "Measurement of the B_c^+ meson lifetime using $B_c^+ \to J/\psi\mu+\nu X$ decays", *JHEP* **74** (2014) 2839, doi:10.1140/epjc/s10052-014-2839-x, arXiv:1401.6932.

[9] LHCb Collaboration, "Measurement of the lifetime of the B_c^+ meson using the $B_c^+ \to J/\psi\pi^+$ decay mode", *Phys. Lett. B* **742** (2015) 29, doi:10.1016/j.physletb.2015.01.010, arXiv:1411.6899.

[10] CDF Collaboration, "Measurement of the B_c^+ meson lifetime using $B_c^+ \to J/\psi e^+\nu_e$", *Phys. Rev. Lett.* **97** (2006) 012002, doi:10.1103/PhysRevLett.97.012002, arXiv:hep-ex/0603027.

[11] CDF Collaboration, "Measurement of the B_c^- meson lifetime in the decay $B_c^- \to J/\psi\pi^-$", *Phys. Rev. D.* **87** (2013) 011101, doi:10.1103/PhysRevD.87.011101, arXiv:1210.2366.

[12] D0 Collaboration, "Measurement of the lifetime of the $B_c^{\pm}$ meson in the semileptonic decay channel", *Phys. Rev. Lett.* **102** (2009) 092001, doi:10.1103/PhysRevLett.102.092001, arXiv:0805.2614.

[13] CMS Collaboration, "Description and performance of track and primary-vertex reconstruction with the CMS tracker", *JINST* **9** (2014) P10009, doi:10.1088/1748-0221/9/10/P10009, arXiv:1405.6569.

[14] T. Sjöstrand, S. Mrenna, and P. Z. Skands, "PYTHIA 6.4 Physics and Manual", *JHEP* **05** (2006) 026, doi:10.1088/1126-6708/2006/05/026, arXiv:hep-ph/0603175.

[15] C. Chang, C. Driouchi, P. Eerola, and X. Wu, "BCVEGPY: an event generator for hadronic production of the B_c meson", *Comput. Phys. Commun.* **159** (2004) 192–224, doi:10.1016/j.cpc.2004.02.005, arXiv:hep-ph/0309120.

[16] J. Chang, C Wang and X. Wu, "BCVEGPY2.0: An upgraded version of the generator BCVEGPY with the addition of hadroproduction of the P-wave B_c states", *Comput. Phys. Commun.* **174** (2006) 241–251, doi:10.1016/j.cpc.2005.09.008, arXiv:hep-ph/0504017.

[17] D. Lange, "The EvtGen particle decay simulation package", *Nucl. Instrum. Meth. A* **462** (2001) 152, doi:10.1016/S0168-9002(01)00089-4.

[18] P. Golonka and Z. Was, "PHOTOS Monte Carlo: a precision tool for QED corrections in Z and W decays", *Eur.Phys.J.C* **45** (2006) 97, doi:10.1140/epjc/s2005-02396-4, arXiv:0506026.

[19] GEANT4 Collaboration, "GEANT4: A Simulation toolkit", *Nucl. Instrum. Meth. A* **506** (2003) 250, doi:10.1016/S0168-9002(03)01368-8.

[20] CMS Collaboration, "Performance of CMS muon reconstruction in pp collision events at $\sqrt{s} = 7$ TeV", *JINST* **7** (2012) P10002, doi:10.1088/1748-0221/7/10/P10002, arXiv:1206.4071.

[21] CMS Collaboration, "CMS tracking performance results from early LHC operation", *Eur. Phys. J. C* **70** (2010) 1165, doi:10.1140/epjc/s10052-010-1491-3, arXiv:1007.1988.

[22] LHCb Collaboration, "First observation of the decay $B_c^+ \to J/\psi\, K^+$", *JHEP* **09** (2013) 075, doi:10.1007/JHEP09(2013)075, arXiv:1306.6723.

[23] T. Skwarnicki, "A study of the radiative CASCADE transitions between the Upsilon-Prime and Upsilon resonances". PhD thesis, Cracow, INP, 1986.

[24] M. J. Oreglia, "A Study of the Reactions $\psi' \to \gamma\gamma\psi$". PhD thesis, SLAC, 1980.

[25] FOCUS Collaboration, "Study of the Cabibbo-suppressed decay mode $D0 \to \pi^-\pi^+$ and $D0 \to K^-K^+$", *Phys. Lett. B* **555** (2003) 167, doi:10.1016/S0370-2693(03)00053-4.